Published in final edited form as:
Cell Death Differ. 2010 May ; 17(5): 821–832. doi:10.1038/cdd.2009.166.

Apoptosis and non-inflammatory phagocytosis can be induced by mitochondrial damage without caspases

Mark F. van Delft[1,2,3], **Darrin P. Smith**[1], **Mireille H. Lahoud**[1], **David C.S. Huang**[1], and **Jerry M. Adams**[1]

[1]The Walter and Eliza Hall Institute of Medical Research, 1G Royal Parade, Parkville, Victoria 3050, Australia.

[2]Department of Medical Biology, University of Melbourne, Melbourne, Australia

Abstract

A central issue regarding vertebrate apoptosis is whether caspase activity is essential, particularly for its crucial biological outcome, non-inflammatory clearance of the dying cell. Caspase-9 is required for the proteolytic cascade unleashed by the mitochondrial outer membrane permeabilization (MOMP) regulated by the Bcl-2 protein family. However, despite the severely blunted apoptosis in cells from *Casp9*$^{-/-}$ mice, some organs with copious apoptosis, such as the thymus, appear unaffected. To address this paradox, we investigated how caspase-9 loss affects apoptosis and clearance of mouse fibroblasts and thymocytes. Although *Casp9*$^{-/-}$ cells were initially refractory to apoptotic insults, they eventually succumbed to slower caspase-independent cell death. Furthermore, in γ-irradiated mice, the dying *Casp9*$^{-/-}$ thymocytes were efficiently cleared, without apparent inflammation. Notably, MOMP proceeded normally, and the impaired mitochondrial function, revealed by diminished mitochondrial membrane potential ($\Delta\psi_m$), committed cells to die, as judged by loss of clonogenicity. Upon the eventual full collapse of $\Delta\psi_m$, presumably reflecting failure of respiration, intact dying *Casp9*$^{-/-}$ cells unexpectedly exposed the prototypic “eat-me” signal phosphatidylserine, which allowed their recognition and engulfment by phagocytes without overt inflammation. Hence, caspase-9-induced proteolysis accelerates apoptosis, but impaired mitochondrial integrity apparently triggers a default caspase-independent program of cell death and non-inflammatory clearance. Thus, caspases appear dispensable for some essential biological functions of apoptosis.

Keywords

apoptosis; mitochondrial membrane potential; Bcl-2 family; caspases; phosphatidylserine

Introduction

The mode of cell death has major biological consequences. Whereas necrosis leads to plasma membrane rupture, release of pro-inflammatory intracellular molecules and collateral tissue damage, apoptosis removes redundant cells and maintains tissue homeostasis in a safe and non-immunogenic manner [1]. It precludes inflammation by confining noxious molecules within intact cell corpses marked for rapid recognition and clearance, typically by professional phagocytes such as macrophages and dendritic cells [2, 3].

CORRESPONDENCE Dr Jerry M. Adams Tel: + 61 3 9345 2555 Fax: +61 3 9347 0852 adams@wehi.edu.au.
[3]Current Address: Division of Cell and Molecular Biology, University Health Network, Toronto, Ontario, M5G 1L7, Canada

Vertebrate apoptosis is regulated primarily by the Bcl-2 protein family [4]. Bcl-2 and close homologs keep the pro-apoptotic mediators Bax and Bak in check until developmental cues or imposed stresses activate the distantly related BH3-only proteins (*e.g.* Bim, Bad, Noxa). Their engagement of pro-survival relatives, and perhaps also Bax or Bak, allows Bax and Bak to oligomerize and permeabilize the mitochondrial outer membrane. The cytochrome *c* released to the cytosol binds Apaf-1, which recruits caspase-9 to form the apoptosome. Caspase-9 can then cleave and activate the effector caspases-3, -6 and -7, which dismantle the cell by cleaving vital intracellular substrates [5]. Exposure on the cell corpse of molecules such as phosphatidylserine (PS) permits its non-inflammatory phagocytosis [2, 3].

Caspases are widely regarded as essential executors of vertebrate apoptosis because mice lacking caspase-9 [6, 7], Apaf-1 [8, 9] or both effector caspases-3 and -7 [10] typically die prior to birth with abnormalities, most notably exencephaly, and their cells are refractory to many apoptotic stimuli. However, hematopoiesis, in which programmed cell death is abundant, appears normal in the absence of caspase-9 or Apaf-1 [11], or both caspases-3 and -7 [10], and tissues with copious apoptosis, such as the thymus, exhibit no inflammation. Thus, the ultimate objective of apoptosis, non-inflammatory cell clearance, might be achievable without caspases.

To investigate this paradox, we have analyzed further how thymocytes and fibroblasts lacking caspase-9 die and are cleared. We find that they die by a caspase-independent cell death mechanism that follows mitochondrial outer membrane permeabilization (MOMP) and diminished mitochondrial membrane potential. Moreover, the cells with damaged mitochondria remained intact and, to our surprise, exposed PS on their surface, allowing their efficient phagocytosis. We conclude that caspase activation accelerates apoptosis but is not strictly required for loss of cell viability or non-inflammatory clearance of the corpses.

Results

Apoptosis is markedly delayed but not ablated in *Casp9*$^{-/-}$ thymocytes

Previous studies differ on the impact of caspase-9 loss on hematopoietic cell death. In short-term assays, cells lacking caspase-9 or Apaf-1 were greatly resistant to apoptotic stimuli [6-9], but a study from this laboratory based largely on *in vitro* assays spanning several days found that they died at rates comparable to wild-type cells [11]. We therefore compared the rates for wild-type, *Casp9*$^{-/-}$ and Bcl-2 transgenic thymocytes in both short- and long-term *in vitro* assays. As initially reported [6, 7], at 24 h *Casp9*$^{-/-}$ thymocytes, unlike the wild-type cells, were largely refractory to γ-irradiation, etoposide, dexamethasone and phorbol myristate acetate (PMA), indeed virtually as resistant as the Bcl-2 transgenic cells (Figs 1A, S1A). In extended assays, however, all these stimuli provoked considerably more death in *Casp9*$^{-/-}$ thymocytes than Bcl-2 transgenic counterparts (Figs 1B, S1B). Similarly, *Casp9*$^{-/-}$ thymocytes cultured *ex vivo* for up to 5 days without cytokines died at later times only moderately slower than wild-type counterparts and more rapidly than the Bcl-2 transgenic cells (Fig 1C). Thus, caspase-9 accelerates the thymocyte death caused by apoptotic stresses but is not essential.

The death of *Casp9*$^{-/-}$ cells does not rely upon residual caspase activation

As expected, the *Casp9*$^{-/-}$ thymocytes exhibited far less caspase activity than the wild-type cells. After γ-irradiation, active caspases were robustly labeled with a biotinylated irreversible caspase inhibitor (biotin-XVAD-fmk) in lysates of wild-type thymocytes but far less so in *Casp9*$^{-/-}$ lysates (Fig 2A). Indeed, quantitative Western blots and fluorogenic substrate assays indicated that the *Casp9*$^{-/-}$ thymocytes had only ~3% as many active caspase molecules as wild-type counterparts (Fig S2). To identify the active caspases, we

isolated the biotinylated polypeptides with streptavidin resin and probed them with specific antibodies. Whereas the wild-type thymocytes yielded active caspases-1, -2, -3, -7, -8, -11, and -12 (Fig 2B), most of which were probably activated by the abundant active caspases-3 and -7, the *Casp9*$^{-/-}$ thymocytes yielded small amounts of active caspases-3 and -7, but no others were detectable (Fig 2B).

To determine whether the residual effector caspase activity drove the death of irradiated *Casp9*$^{-/-}$ thymocytes, we tested the impact of two broad-spectrum caspase inhibitors. Both effectively inhibited apoptosis in wild-type thymocytes but the marginal increase in the viability of the *Casp9*$^{-/-}$ thymocytes was comparable to that in untreated cultured cells (Fig S3A). Hence, neither compound specifically inhibited their γ-irradiation-induced death (Fig 2C), and even their 'spontaneous death' in culture was only slightly delayed by caspase inhibition (Fig S3B). Thus, the death of *Casp9*$^{-/-}$ thymocytes is not attributable to residual active effector caspases.

We also evaluated apoptosis in *Casp9*$^{-/-}$ mouse embryonic fibroblasts (MEFs), using either a cytotoxic stimulus that evokes DNA damage (etoposide) or signals that directly neutralize all of the Bcl-2-like pro-survival proteins [12]: (a) expression of the potent BH3-only protein Bim, or (b), exposure of cells over-expressing the selective BH3-only protein Noxa to the Bad-like BH3 mimetic ABT-737 13. In short-term assays, *Casp9*$^{-/-}$ MEFs were refractory to all three insults (Fig S4A) and their death was modest even over several days (Fig S4B). Moreover, no substantial effector caspase activation was evident in the *Casp9*$^{-/-}$ MEFs (Fig S4C), and broad-spectrum caspase inhibitors did not block their death (Fig S4D). Thus, like the mutant thymocytes, the *Casp9*$^{-/-}$ MEFs died slowly by a caspase-independent pathway.

The different apoptotic stages regulated by Bcl-2 and caspases are discernable by mitochondrial membrane potential

Bcl-2 preserves mitochondrial integrity and hence function, whereas caspase-9 acts downstream of MOMP. To assess mitochondrial function during apoptosis, we used the potentiometric dye 3,3′dihexyloxacarbocyanine iodide ($DiOC_6(3)$) to monitor changes in mitochondrial membrane potential ($\Delta\psi_m$), a hydrogen ion gradient across the inner membrane that is coupled to oxidative phosphorylation [14].

We first compared wild-type and *Casp9*$^{-/-}$ MEFs, *Casp9*$^{-/-}$ MEFs stably overexpressing Bcl-2, and MEFs lacking the essential pro-apoptotic proteins Bax and Bak. Each initially displayed a small transient increase in $\Delta\psi_m$ [15], which was complete within 2 h (Fig S5). Their subsequent $\Delta\psi_m$ depended on their genetic constitution. Wild-type MEFs lost $\Delta\psi_m$ completely within 48 h, and their plasma membranes concomitantly became permeable, as detected by propidium iodide (PI) uptake (Fig 3A). Thus, over time, the viable (PI^{-ve}) wild-type cells, shown by filled histograms, were replaced by dead (PI^{+ve}) cells, shown by the unfilled histograms. In contrast, most *Casp9*$^{-/-}$ MEFs remained intact, and unexpectedly acquired an intermediate $\Delta\psi_m$, which was maintained in the majority of cells for at least 48 h in Fig 3A and at least 72 h in another experiment (data not shown). Bcl-2 overexpression in the *Casp9*$^{-/-}$ MEFs prevented this initial $\Delta\psi_m$ decline, as did the absence of both Bax and Bak (Fig 3A). In contrast, broad-spectrum caspase inhibitors failed to prevent the initial $\Delta\psi_m$ drop in either the wild-type or *Casp9*$^{-/-}$ MEFs but did prevent the further $\Delta\psi_m$ collapse in the wild-type MEFs (Fig 3B).

Similarly, in γ-irradiated thymocytes, Bcl-2 over-expression prevented the initial fall in $\Delta\psi_m$, whereas caspase-9 loss or caspase inhibition prevented only the further complete loss of $\Delta\psi_m$ (Fig 3C). The thymocytes were less robust than the MEFs. At 24 h after irradiation only 38% of the *Casp9*$^{-/-}$ thymocytes persisted with an intermediate $\Delta\psi_m$ (Fig 3C), and by 48 h only 20% remained viable (data not shown).

We hypothesized that the initial drop in $\Delta\psi_m$ resulted from MOMP and that the rapid subsequent $\Delta\psi_m$ collapse in the wild-type cells was caspase-mediated (Fig. 3D). Indeed, a flow cytometric sort of stressed MEFS by $\Delta\psi_m$ revealed that cytochrome *c* had been released in cells with intermediate $\Delta\psi_m$ but not those retaining high $\Delta\psi_m$ (Fig 4A). Furthermore, when we neutralized all the Bcl-2 pro-survival proteins in Casp9−/− MEFs with Noxa plus ABT-737, cytochrome c release preceded the drop to intermediate $\Delta\psi_m$ by 0.5 h (Fig 4B).

Thus, $\Delta\psi_m$ decreases in two discrete steps during apoptosis (Fig 3D). The intermediate $\Delta\psi_m$ results from MOMP, since that decline requires pro-apoptotic Bax or Bak but not caspases, is inhibited by Bcl-2 and shortly follows cytochrome *c* release. The later complete collapse of $\Delta\psi_m$ (depolarisation) probably reflects cessation of respiration (see Discussion), and its acceleration in the wild-type cells may well reflect destruction of electron transport components by effector caspases [16].

MOMP commits the cells to die

To determine whether MOMP commits the cells to die, we first exposed *Casp9*$^{-/-}$ MEFs expressing Noxa to graded concentrations of ABT-737 and measured both $\Delta\psi_m$ and clonogenic potential. Indeed, the drop to an intermediate $\Delta\psi_m$ correlated strongly with reduced colony formation (Fig 5A). Moreover, when we sorted the stressed MEFs by $\Delta\psi_m$, those retaining high $\Delta\psi_m$ formed colonies comparably to untreated cells, whereas those of intermediate $\Delta\psi_m$ yielded none (Fig 5B). The common apoptotic stimulus staurosporine gave equivalent results (Fig S6). Thus, MOMP commits MEFs to die, as reported for immortal hematopoietic cells and mast cells [17, 18].

The impaired mitochondrial function (Fig 3) and loss of clonogenicity (Fig 5) in the stressed *Casp9*$^{-/-}$ cells can explain why over-expressed Bcl-2 but not caspase-9 loss prolongs lymphocyte survival *in vivo* [11]. But if *Casp9*$^{-/-}$ cells do not undergo caspase-dependent apoptosis, how are they properly cleared from the animal?

Dying *Casp9*$^{-/-}$ thymocytes are efficiently cleared by phagocytes *in vivo*

Non-inflammatory clearance of wild-type cells is ensured by their exposure of PS [2, 3]. Genetic lesions or agents that interfere with PS-mediated clearance lead within six weeks to anti-nuclear autoantibodies in the serum, perhaps because secondary necrosis of the lingering cells creates a pro-inflammatory milieu that breaks self-tolerance [19, 20]. However, no anti-nuclear antibodies appeared in the sera of mice up to 20 weeks after reconstitution with *Casp9*$^{-/-}$ hematopoietic stem cells (Fig S7). This finding, combined with the normal cellular composition and lack of inflammation in hematopoietic organs [11], suggests that dying *Casp9*$^{-/-}$ cells must be removed appropriately.

To test directly whether *Casp9*$^{-/-}$ cells are efficiently cleared *in vivo*, we monitored thymocyte cell death and clearance from reconstituted mice exposed to whole-body γ-irradiation, which decimates the wild-type thymus. Whereas wild-type thymocytes, particularly the exquisitely sensitive $CD4^+CD8^+$ cells, plummeted in number, the loss of *Casp9*$^{-/-}$ thymocytes was delayed (Fig 6A, 6B). Nevertheless, by 24 h, ~85% of them had been successfully cleared (Fig 6A), and histological sections of both *Casp9*$^{-/-}$ and wild-type thymi revealed dramatically fewer lymphocytes (Fig 6C). Moreover, the proportion of thymic $TUNEL^{+ve}$ macrophages ($CD11b^{+ve}$), *i.e.* those that have engulfed apoptotic thymocytes [21], increased substantially following irradiation of both wild-type and *Casp9*$^{-/-}$ reconstituted animals (Fig 6D). Hence, *Casp9*$^{-/-}$thymocytes must still display signals that promote their phagocytosis.

Dying *Casp9*$^{-/-}$ thymocytes display PS before they lose plasma membrane integrity

PS, detected by staining with Annexin V, is the best characterized molecule that marks apoptotic cells for phagocytosis [3]. Its exposure is widely thought to be caspase-dependent [5, 22], although there are reported examples of caspase-independent PS translocation [3, 23-25]. Indeed, we noted that even though *Casp9*$^{-/-}$ cells die with little or no caspase contribution (Figs 2, S2, S3), they still exposed PS before losing plasma membrane integrity, *i.e.* becoming PI^{+ve} (Fig 7A). Furthermore, a broad-spectrum caspase inhibitor did not block the PS exposure (Fig 7B). Caspase activity is not, therefore, essential for intact dying cells to expose PS. Like cells undergoing conventional apoptosis, at any one time, only a small proportion of the cells (~5-10%) were Annexin V^{+ve} PI^{-ve}, but it seems likely that most or all pass through that state.

Interestingly, we identified a striking association between PS exposure and $\Delta\psi_m$ collapse. Staining simultaneously for plasma membrane integrity (with PI), $\Delta\psi_m$ and PS exposure revealed that nearly all wild-type and *Casp9*$^{-/-}$ cells with intact plasma membranes and exposed PS had lost $\Delta\psi_m$, as indicated by the PI^{-ve}AnnexinV^{+ve} (green) population (Figs 7C, 7D). Conversely, all the cells with an intact plasma membrane that lacked exposed PS, namely the PI^{-ve}AnnexinV^{-ve} (blue) population, displayed either full or intermediate $\Delta\psi_m$. Thus, in both *Casp9*$^{-/-}$ and wild-type cells, PS exposure is tightly correlated with collapse of $\Delta\psi_m$. Because the PS exposure precedes the loss of plasma membrane integrity, it may well flag the intact corpses for efficient non-inflammatory clearance *in vivo*.

Phagocytes recognize and engulf only *Casp9*$^{-/-}$ cells that expose PS

Two other signals on some dying wild-type cells that influence phagocytosis are exposure of the "eat-me" signal calreticulin and reduced expression of the "don't-eat-me" signal CD47 [26], although whether these alterations require caspases or are linked to PS exposure is unknown. We tested whether dying *Casp9*$^{-/-}$ cells (*i.e.* those that have undergone MOMP and thus cannot proliferate but have not yet exposed PS – designated hereafter as "moribund") exhibited these changes. Neither signal, however, discriminated between moribund and healthy *Casp9*$^{-/-}$ cells. Whereas apoptotic wild-type cells exposed calreticulin on their surface [26], moribund *Casp9*$^{-/-}$ cells did not (Fig 8A). Likewise, whereas apoptotic wild-type cells had reduced expression of CD47, moribund *Casp9*$^{-/-}$ cells maintained normal levels, and it remained fully competent to bind its phagocyte receptor SIRPα (Fig 8A). These differences suggest that both the exposure of calreticulin and reduced surface CD47 expression on apoptotic cells are directly or indirectly provoked by caspase activity. Moreover, these changes must either coincide with or occur downstream of PS exposure.

To test functionally whether PS exposure was critical for phagocytosis of dying *Casp9*$^{-/-}$ cells, we adopted an *in vitro* assay, using as targets irradiated thymocytes labeled with the dye carboxy-fluorescein diacetate succinimidyl ester (CFSE). We first confirmed that macrophages engulfed in a temperature-dependent manner not only apoptotic wild-type cells but also *Casp9*$^{-/-}$ thymocytes, albeit less efficiently (Figs 8B, 8C). Significantly, however, irradiated *Casp9*$^{-/-}$ thymocytes bearing surface PS were phagocytosed as efficiently as wild-type counterparts, whereas the moribund PS^{-ve} cells were as refractory to engulfment as healthy PS^{-ve} cells (Fig 8D). We conclude that *Casp9*$^{-/-}$ cells are engulfed when they have redistributed PS to their surface, and thus that surface PS represents a critical signal for their clearance.

Discussion

The paramount function of apoptosis is to remove redundant cells without inducing inflammation [1]. We have examined how loss of caspase-9, a critical component of the intrinsic apoptotic pathway, impacts on that function. Although nearly all hallmarks of apoptosis are ascribed to caspases [5], blocking their action has surprisingly limited effects in the animal. The defects in embryos lacking caspase-9, Apaf-1, or both effector caspases -3 and -7 are confined to select organs [6-10]. Remarkably, the mutant hematopoietic organs, including those with abundant apoptosis such as the thymus, exhibit normal cellularity and composition [10, 11].

An earlier study from our laboratory noted the residual caspase activity in dying *Casp9*$^{-/-}$ cells and hypothesized that alternative Bcl-2-regulated initiator caspases might still drive caspase-dependent apoptosis 11. That hypothesis now appears unlikely, because lymphocytes are not elevated by the knockout of any individual initiator caspase, nor even the combined loss of caspases 2 and 9 [27], or caspases 1, 11 and 9 (DPS, MFvD and JMA, unpublished results), whereas lymphopoiesis is grossly perturbed when MOMP is blocked by the absence of both Bax and Bak [28] or by Bcl-2 over-expression 11. Furthermore, we detected no active initiator caspase in irradiated *Casp9*$^{-/-}$ thymocytes (Fig 2B). Traces of active effector caspase-3 and -7 were detected, but pharmacological inhibition argues against a crucial role for them in the demise (Figs 2C, S3B) or clearance (Fig 7B) of the *Casp9*$^{-/-}$ cells. Because pro-caspase-3 autoactivates when the pH is lowered [29], the MOMP-induced acidification of the cytosol [30] may produce the traces of active effector caspases.

Model for caspase-independent cell death and clearance

As Figure 9 outlines, our findings suggest that *Casp9*$^{-/-}$ cells exposed to apoptotic stimuli die by caspase-independent cell death following the mitochondrial damage controlled by the Bcl-2 family (Figs 3 - 5). MOMP may promote caspase-independent cell death through generation of reactive oxygen species, depletion of ATP or other metabolic dysfunctions [22].

Monitoring $\Delta\psi_m$ during apoptosis of genetically modified cells revealed two discrete phases of mitochondrial damage. The initial drop to an intermediate $\Delta\psi_m$ results from MOMP, as it was mediated by Bax/Bak but not caspases (Fig 3) and shortly followed cytochrome *c* release (Fig 4). Importantly, as reported for two other cell types [17, 18], MOMP committed the cells to die, as they no longer formed colonies (Figs 5, S6), although their plasma membranes remained intact. The second phase of mitochondrial damage, hastened in wild-type cells by activated caspases [16], ablated $\Delta\psi_m$ (Fig 3). The reduced $\Delta\psi_m$ following MOMP might not be expected, because $\Delta\psi_m$ reflects a hydrogen ion gradient across the inner mitochondrial membrane, and the channels in the outer membrane (*e.g.* VDAC) are thought to be porous to hydrogen ions. Since the residual cytochrome *c* remaining in mitochondria by diffusion after MOMP limits oxidative phosphorylation [31], the intermediate $\Delta\psi_m$ probably reflects reduced ATP production, whereas its total collapse probably reflects failure of respiration (Fig 9).

We found that dying *Casp9*$^{-/-}$ cells exposed PS while they remained intact (Fig 7), allowing their efficient phagocytosis (Figs 6 and 8) without release of noxious molecules. The PS exposure coincided with $\Delta\psi_m$ collapse, in both the wild-type cells dying rapidly by caspase-dependent apoptosis and the *Casp9*$^{-/-}$ cells dying more slowly by a caspase-independent mechanism (Figs 7C, 7D). This suggests that the same underlying mechanism may be engaged and that collapse of $\Delta\psi_m$ (*i.e.* respiratory failure) triggers PS exposure (Fig 9).

How $\Delta\psi_m$ collapse provokes PS exposure remains uncertain. However, since the translocase that shifts PS from the outer to the inner leaflet of the plasma membrane requires ATP [2], one

appealing possibility is that the lower ATP production following MOMP [31] reduces translocase activity, allowing PS accumulation in the outer leaflet [25, 32]. Reduced cellular ATP presumably would also impair plasma membrane Ca^{2+} ATPase function, leading to Ca^{2+} influx and activation of the "scramblase" thought to flip PS bi-directionally between the outer and inner leaflets of the plasma membrane [3]. However, the identity and role of scamblases remains uncertain [32] and a very recent study has suggested that exposed PS may derive instead from fusion of lysosomes with the plasma membrane [33]. In any case, dying cells that quickly expose PS on their surface as a consequence of caspase activation and those that do so after a lag, probably as a result of respiratory failure, were equally able to recruit phagocytes and induce engulfment of the intact cell corpse (Figs 8C, 9). Other signals that contribute to phagocytosis of wild-type cells, such as calreticulin exposure and down regulation of CD47 [26], likely accelerate the process when caspases are active but do not precede PS exposure in moribund *Casp9*$^{-/-}$ cells (Fig 8A).

Implications of caspase-independent cell death

Our findings suggest that caspase activation in the intrinsic apoptotic pathway is not absolutely required for either cell death or non-inflammatory clearance. Indeed, the overall pathways *in vivo* in its absence and presence appear remarkably similar (Fig 9): both are triggered by MOMP, proceed through loss of $\Delta\psi_m$ and induce PS exposure to allow efficient phagocytosis without overt inflammation. The only obvious consequence of precluding caspase activation for thymocytes *in vivo* was the lag in their elimination (Fig 6), presumably reflecting a slow attrition in $\Delta\psi_m$ and respiration (Fig 9). The caspase-deficient cells are then most likely demolished in a non-cell autonomous fashion within the phagocyte [20].

We suggest that the primary role of caspases in vertebrates is to accelerate the cell death process. Punctual cell removal undoubtedly is essential to eliminate infected cells to limit spread of the infection, as well as to sculpt certain developing tissues, as exemplified by the exencephaly in *Casp9*$^{-/-}$ embryos. For many other important cell death programs, however, such as T cell selection in the thymus, the somewhat slower MOMP-driven pathway to PS exposure apparently allows effective clearance, seemingly without inflammation or autoimmunity (Fig 9). Vertebrates may have evolved this caspase-independent cell death program as a fail-safe to eliminate cells deficient in mitochondrial function, whether due to MOMP or other types of mitochondrial damage.

Defects in clearance or degradation of apoptotic cell components can cause autoimmune disease, anemia and chronic arthritis [20]. More controversially, certain tumors reportedly exhibit alterations that would impair apoptosis downstream of MOMP, such as loss of Apaf-1 expression, perhaps implicating impaired caspase-independent cell death in their evolution [22]. Such alterations might hamper responses to cancer therapy, because the higher glycolysis in many tumor cells would render them less dependent on mitochondrial function than normal cells [34] and hence more refractory to MOMP-driven death and clearance. Eradicating the most resistant tumor cells might therefore require augmenting caspase activation, *e.g.* by targeting both the intrinsic (mitochondrial) and the extrinsic (death receptor) pathways, or enhancing their phagocytosis by devising ways to promote PS exposure, such as reducing their ATP levels [25] by inhibiting glycolysis. Another avenue of attack is opened by recent evidence that certain leukemia cells evade phagocytosis and persist by not down regulating CD47, since their clearance can be enhanced with blocking CD47 antibodies 35, 36. Thus, further clarification of cell clearance mechanisms should impact on the treatment of several major diseases.

Materials and Methods

Mice

The *vav-Bcl-2* mice [37] were generated on an inbred C57BL/6 background while *Casp9*$^{+/-}$ mice [7], originally generated on a mixed C57BL/6/129SV background, were backcrossed for >12 generations to C57BL/6 mice prior to intercrossing for these experiments. To circumvent the perinatal lethality of embryos lacking caspase-9, fetal liver stem cells from *Casp9*$^{-/-}$ and *Casp9*$^{+/+}$ E14.5 embryos (on a C57BL/6-Ly5.2 background) were used to reconstitute hematopoiesis in irradiated (2 × 5.5 Gy) C57BL/6-Ly5.1 recipient mice as described [11]. Thymi were harvested 11-15 weeks post-reconstitution, at which point thymocyte suspensions typically comprised > 99% donor-derived Ly5.2^{+ve} cells as determined by FACS analysis.

Cell culture

All cells were cultured in DMEM supplemented with 250 μM asparagine, 50 μM 2-mercaptoethanol and 10% fetal calf serum. Single-cell thymocyte suspensions were prepared by passing thymus tissue through a fine wire mesh and the cells immediately cultured (at 1 × 10^6 cells/mL) without further manipulation. *WT* and *Casp9*$^{-/-}$ MEFs were immortalized by a 3T9 culture protocol [38]. MEFs stably expressing Bcl-2 were generated by electroporation (Bio-Rad) of an expression plasmid (pEF Flag-Bcl2/puro) [39] and selection of puromycin-resistant clones, which were shown to overexpress Bcl-2 by FACS analysis. The *Bax*$^{-/-}$/*Bak*$^{-/-}$ MEF cell line was a gift from the late Dr. S.J. Korsmeyer and the J774 macrophage cell line from the late Dr. A.W. Harris.

Cell Death Assays

Apoptosis was induced in cultured thymocytes by exposure to the indicated doses of γ-irradiation (from a ^{60}Co source) or concentrations of etoposide (Pharmacia), dexamethasone (Sigma) or PMA (Sigma). Apoptosis was induced in MEF cultures by exposure to the indicated concentrations of etoposide, staurosporine (Sigma) or ABT-737 13, or by retroviral expression of BH3-only proteins as described 12. Cell viability was determined by staining the cells with 1 μg/mL PI followed by FACS analysis. The caspase inhibitors IDN-6275 40 (gift of Drs. K. Tomaselli and T. Oltersdorf) and zVAD-fmk (Bachem) were dissolved in DMSO and added at 50 μM to cultures 1-2 h prior to exposure to the apoptotic stimulus. Clonogenic assays were performed by plating equal numbers of cells in separate wells, culturing them for 7 days and revealing macroscopic colonies by staining with Giemsa (Sigma).

Flow Cytometric Analyses and Cell Sorting

Cell suspensions were stained in balanced salt solution containing 2% fetal calf serum, plus 1% rat serum when staining thymocytes. For surface staining of adherent MEF, the cells were suspended with PBS-based enzyme-free cell dissociation buffer (GIBCO). Antibodies were obtained commercially or purified from hybridoma supernatant and conjugated in our laboratory by Dr. A. Strasser. They included: anti-CD4-biotin (H129), anti-CD8-FITC (YTS169), anti-CD11b-APC (MI/70, Pharmingen), anti-CD47 (miap301, Pharmingen) and anti-calreticulin (SPA-600, Stressgen). CD4-biotin was detected with streptavidin-PE (Caltag), CD47 with goat-anti-rat-IgG-FITC (Southern Biotech), and calreticulin staining with goat-anti-rabbit-IgG-FITC (Southern Biotech). Annexin V-FITC and Annexin V-biotin were conjugated in our laboratory by Dr. A. Strasser. Annexin V-biotin staining was detected with streptavidin-APC (Caltag). Soluble SIRPα ectodomian was produced by transfection of 293T cells with a construct encoding a fusion of the SIRPα ectodomain with the rat CD4 domains 3 and 4 and a biotinylation consensus sequence [41]. The recombinant

protein was biotinylated using the *E. coli* enzyme BirA (Avidity) and binding detected using Streptavidin-PE (Caltag).

To assess $\Delta\psi_m$, cells were cultured in media containing 40 nM $DiOC_6(3)$ for 15 min at 37 °C, harvested, placed on ice and analyzed within 1 h. TUNEL staining was performed with the fluorescein In Situ Cell Death Detection Kit (Roche) following the manufacturer's protocol. Cytochrome *c* release was visualized as described [42]. Stained cells were analyzed on a FACScan (Becton Dickinson) or FACSCalibur (Becton Dickinson), and cell populations isolated using a MoFlo cell sorter (Cytomation).

Phagocytosis Assays

J774 macrophages were plated at 1×10^5 cells/well in 24-well plates and cultured overnight. Thymocytes were labeled with 2.5 μM CFSE for 7 min at room temperature in balanced salt solution, washed, resuspended in culture medium, either left untreated or exposed to 5 Gy γ-irradiation, and then cultured for 24 h. Prior to co-culture, the untreated thymocytes were centrifuged over Ficoll-Paque Plus (Pharmacia) to enrich for viable (Ficoll-buoyant) cells, which were washed and resuspended in culture medium. Their viability was then typically >90%, whereas 24 h after γ-irradiation wild-type and *Casp9*$^{-/-}$ thymocytes were typically ~10% and ~70% viable, respectively. 2×10^6 CFSE-labeled thymocytes were added to each well of macrophages and co-cultured for 1 h at 37 °C or on ice. Macrophages were then washed with PBS to remove uningested thymocytes, resuspended with trypsinization and analyzed by flow cytometry. In the experiment using enriched fractions of thymocytes as targets (Fig 8D), untreated and γ-irradiated CFSE-labeled thymocytes were stained with PI and sorted into PI^{+ve} and PI^{-ve} fractions. The fractions designated "healthy" were PI^{-ve} thymocytes sorted from untreated samples, most of which have high $\Delta\psi_m$ (*e.g.* see Figs 7C, 7D). The "apoptotic" fractions were PI^{+ve} thymocytes sorted from irradiated samples, which have low $\Delta\psi_m$ (*e.g.* see Figs 7C, 7D). The "moribund" fractions were PI^{-ve} thymocytes sorted from irradiated *Casp9*$^{-/-}$ thymocytes, which primarily have intermediate $\Delta\psi_m$ (*e.g.* see Fig 7D). The "healthy" and "moribund" fractions both contained a minor contaminating population (< 10%) of PS^{+ve} cells, which likely contributed to the background levels of phagocytosis for these fractions.

Antinuclear Antibody Detection by Indirect Immunofluorescence

Serum samples were diluted 1:100 with PBS and added to glass slides coated with HEp-2 cells (Cedarlane Diagnostics). The slides were incubated at room temperature in a humid chamber for 30 min. Antibodies bound to the slides were detected by staining with FITC-conjugated goat anti–mouse IgG (Southern Biotechnology). Slides were observed with a Zeiss Axioplan 2 fluorescence microscope and images captured using a Zeiss Axiocam and Axiovision software (Carl Zeiss).

Histology and Microscopic Imaging

Thymus tissue was fixed in Bouin's, sectioned, and stained with haematoxylin and eosin. The sections were observed using an Optiphot microscope (Nikon) with a Plan Apo × 100 (NA 1.35, oil) objective lens and images were captured with a Nikon DS camera head (DS-5M) and control unit (DS-L1) using integral software.

Measurements of Caspase Activity

Cell lysates were prepared in TNE lysis buffer (50 mM Tris pH 7.5, 150 mM NaCl, 2 mM EDTA, 1% NP-40, 1X complete protease inhibitors (Roche), 5 mM DTT). The active caspases were labeled by exposure to 2.5 μM biotin-XVAD-fmk (gift of Drs. D. Nicholson and S. Roy) for 30 min at 37 °C. The labeled caspases were either analyzed in bulk by

western blotting with HRP-conjugated streptavidin or first purified with streptavidin-sepharose resin (Amersham Biosciences), and then analyzed by western blotting with antibodies recognizing active caspase-3 (Chemicon), caspase-7 (1-1-11; gift of Dr. Y. Lazebnik), caspase-1 (1H11; Alexis), caspase-8 [43] (1G12; Alexis), caspase-11 (4E11; Alexis) and caspase-12 (11F10; Alexis). For substrate assays, the lysates were assayed using Rhodamine110 Enz-Check Caspase Assay Kits (Molecular Probes) according to the manufacturers instructions with a SpectraFluor Plus plate reader (TECAN).

Supplementary Material

Refer to Web version on PubMed Central for supplementary material.

Acknowledgments

We thank Professor A. Strasser for discussions and valuable comments on the manuscript; V. Marsden, L O'Reilly, S. Jones, and B. Sheikh for reagents and advice; and G. Siciliano, D. Cooper, K. Pioch and K. Vella for animal care. DNA constructs encoding the soluble SIRPα ectodomain were kindly donated by Assoc. Prof. Mark Wright (Monash University, Melbourne, Australia). This work was supported by a Melbourne University International Research Scholarship and Cancer Council Victoria Postdoctoral Research Fellowship to MvD, National Health and Medical Research Council (NHMRC) Fellowships to DCSH and JMA, and grants from the NHMRC (Program Grant 461221), the NIH (CA43540) and the Leukemia and Lymphoma Society (SCOR grant 7413). Infrastructure support from NHMRC IRIISS grant 361646 and the Victorian State Government OIS grant is gratefully acknowledged.

Abbreviations used

CFSE	carboxy-fluorescein diacetate succinimidyl ester
DiOC$_6$(3)	3,3′dihexyloxacarbocyanine iodide
$\Delta\psi_m$	mitochondrial membrane potential
MEF	mouse embryo fibroblast
MOMP	mitochondrial outer membrane permeabilization
PI	propidium iodide
PS	phosphatidylserine

References

1. Kerr JFR, Wyllie AH, Currie AR. Apoptosis: a basic biological phenomenon with wide-ranging implications in tissue kinetics. British Journal of Cancer 1972;26:239–257. [PubMed: 4561027]
2. Ravichandran KS, Lorenz U. Engulfment of apoptotic cells: signals for a good meal. Nat Rev Immunol 2007;7(12):964–74. [PubMed: 18037898]
3. Schlegel RA, Williamson P. Phosphatidylserine, a death knell. Cell Death Differ 2001;8(6):551–63. [PubMed: 11536005]
4. Adams JM, Cory S. The Bcl-2 apoptotic switch in cancer development and therapy. Oncogene 2007;26(9):1324–1337. [PubMed: 17322918]
5. Taylor RC, Cullen SP, Martin SJ. Apoptosis: controlled demolition at the cellular level. Nat Rev Mol Cell Biol 2008;9(3):231–41. [PubMed: 18073771]
6. Hakem R, Hakem A, Duncan GS, Henderson JT, Woo M, Soengas MS, et al. Differential requirement for caspase 9 in apoptotic pathways in vivo. Cell 1998;94(3):339–352. [PubMed: 9708736]
7. Kuida K, Haydar TF, Kuan CY, Gu Y, Taya C, Karasuyama H, et al. Reduced apoptosis and cytochrome c-mediated caspase activation in mice lacking caspase 9. Cell 1998;94(3):325–37. [PubMed: 9708735]

8. Cecconi F, Alvarez-Bolado G, Meyer BI, Roth KA, Gruss P. Apaf-1 (CED-4 homologue) regulates programmed cell death in mammalian development. Cell 1998;94:727–737. [PubMed: 9753320]
9. Yoshida H, Kong Y-Y, Yoshida R, Elia AJ, Hakem A, Hakem R, et al. Apaf1 is required for mitochondrial pathways of apoptosis and brain development. Cell 1998;94(6):739–750. [PubMed: 9753321]
10. Lakhani SA, Masud A, Kuida K, Porter GA Jr. Booth CJ, Mehal WZ, et al. Caspases 3 and 7: key mediators of mitochondrial events of apoptosis. Science 2006;311(5762):847–851. [PubMed: 16469926]
11. Marsden V, O'Connor L, O'Reilly LA, Silke J, Metcalf D, Ekert P, et al. Apoptosis initiated by Bcl–2-regulated caspase activation independently of the cytochrome c/Apaf–1/caspase–9 apoptosome. Nature 2002;419:634–637. [PubMed: 12374983]
12. Chen L, Willis SN, Wei A, Smith BJ, Fletcher JI, Hinds MG, et al. Differential targeting of pro-survival Bcl-2 proteins by their BH3-only ligands allows complementary apoptotic function. Mol. Cell 2005;17:393–403. [PubMed: 15694340]
13. Oltersdorf T, Elmore SW, Shoemaker AR, Armstrong RC, Augeri DJ, Belli BA, et al. An inhibitor of Bcl-2 family proteins induces regression of solid tumours. Nature 2005;435(7042):677–681. [PubMed: 15902208]
14. Zamzami N, Marchetti P, Castedo M, Zanin C, Vayssiere JL, Petit PX, et al. Reduction in mitochondrial potential constitutes an early irreversible step of programmed lymphocyte death *in vivo*. Journal of Experimental Medicine 1995;181(5):1661–1672. [PubMed: 7722446]
15. Vander Heiden MG, Chandel NS, Williamson EK, Schumacker PT, Thompson CB. Bcl-x_L regulates the membrane potential and volume homeostasis of mitochondria. Cell 1997;91(5):627–637. [PubMed: 9393856]
16. Ricci JE, Munoz-Pinedo C, Fitzgerald P, Bailly-Maitre B, Perkins GA, Yadava N, et al. Disruption of mitochondrial function during apoptosis is mediated by caspase cleavage of the p75 subunit of complex I of the electron transport chain. Cell 2004;117(6):773–786. [PubMed: 15186778]
17. Ekert PG, Read SH, Silke J, Marsden VS, Kaufmann H, Hawkins CJ, et al. Apaf-1 and caspase-9 accelerate apoptosis, but do not determine whether factor-deprived or drug-treated cells die. J Cell Biol 2004;165(6):835–842. [PubMed: 15210730]
18. Marsden VS, Kaufmann T, O'Reilly LA, Adams JM, Strasser A. Apaf-1 and Caspase-9 are required for cytokine withdrawal-induced apoptosis of mast cells but dispensable for their functional and clonogenic death. Blood 2006;107(5):1872–1877. [PubMed: 16291596]
19. Asano K, Miwa M, Miwa K, Hanayama R, Nagase H, Nagata S, et al. Masking of phosphatidylserine inhibits apoptotic cell engulfment and induces autoantibody production in mice. J Exp Med 2004;200(4):459–67. [PubMed: 15302904]
20. Nagata S. Autoimmune diseases caused by defects in clearing dead cells and nuclei expelled from erythroid precursors. Immunol Rev 2007;220:237–50. [PubMed: 17979851]
21. Surh CD, Sprent J. T-cell apoptosis detected *in situ* during positive and negative selection in the thymus. Nature 1994;372:100–103. [PubMed: 7969401]
22. Tait SW, Green DR. Caspase-independent cell death: leaving the set without the final cut. Oncogene 2008;27(50):6452–61. [PubMed: 18955972]
23. Verhoven B, Krahling S, Schlegel RA, Williamson P. Regulation of phosphatidylserine exposure and phagocytosis of apoptotic T lymphocytes. Cell Death and Differentiation 1999;6(3):262–270. [PubMed: 10200577]
24. Ferraro-Peyret C, Quemeneur L, Flacher M, Revillard JP, Genestier L. Caspase-independent phosphatidylserine exposure during apoptosis of primary T lymphocytes. J Immunol 2002;169(9):4805–10. [PubMed: 12391190]
25. Hirt UA, Leist M. Rapid, noninflammatory and PS-dependent phagocytic clearance of necrotic cells. Cell Death Differ 2003;10(10):1156–64. [PubMed: 14502239]
26. Gardai SJ, McPhillips KA, Frasch SC, Janssen WJ, Starefeldt A, Murphy-Ullrich JE, et al. Cell-surface calreticulin initiates clearance of viable or apoptotic cells through trans-activation of LRP on the phagocyte. Cell 2005;123(2):321–34. [PubMed: 16239148]

27. Marsden VS, Ekert PG, Van Delft M, Vaux DL, Adams JM, Strasser A. Bcl-2-regulated apoptosis and cytochrome c release can occur independently of both caspase-2 and caspase-9. J Cell Biol 2004;165(6):775–780. [PubMed: 15210727]
28. Rathmell JC, Lindsten T, Zong W-X, Cinalli RM, Thompson CB. Deficiency in Bak and Bax perturbs thymic selection and lymphoid homeostasis. Nature Immunology 2002;3(10):932–939. [PubMed: 12244308]
29. Roy S, Bayly CI, Gareau Y, Houtzager VM, Kargman S, Keen SL, et al. Maintenance of caspase-3 proenzyme dormancy by an intrinsic “safety catch” regulatory tripeptide. Proceedings of the National Academy of Sciences of the USA 2001;98(11):6132–6137. [PubMed: 11353841]
30. Matsuyama S, Llopis J, Deveraux QL, Tsien RY, Reed JC. Changes in intramitochondrial and cytosolic pH: early events that modulate caspase activation during apoptosis. Nature Cell Biology 2000;2(6):318–325.
31. Waterhouse NJ, Goldstein JC, von Ahsen O, Schuler M, Newmeyer DD, Green DR. Cytochrome c maintains mitochondrial transmembrane potential and ATP generation after outer mitochondrial membrane permeabilization during the apoptotic process. J Cell Biol 2001;153(2):319–28. [PubMed: 11309413]
32. Gleiss B, Gogvadze V, Orrenius S, Fadeel B. Fas-triggered phosphatidylserine exposure is modulated by intracellular ATP. FEBS Lett 2002;519(1-3):153–8. [PubMed: 12023035]
33. Mirnikjoo B, Balasubramanian K, Schroit AJ. Suicidal Membrane Repair Regulates Phosphatidylserine Externalization during Apoptosis. J Biol Chem 2009;284(34):22512–6. [PubMed: 19561081]
34. Colell A, Ricci JE, Tait S, Milasta S, Maurer U, Bouchier-Hayes L, et al. GAPDH and Autophagy Preserve Survival after Apoptotic Cytochrome c Release in the Absence of Caspase Activation. Cell 2007;129(5):983–997. [PubMed: 17540177]
35. Jaiswal S, Jamieson CHM, Pang WW, Park CY, Chao MP, Majeti R, et al. CD47 is upregulated on circulating hematopoietic stem cells and leukemia cells to avoid phagocytosis. Cell 2009;138:271–285. [PubMed: 19632178]
36. Majeti R, Chao MP, Alizadeh AA, Pang WW, Jaiswal S, Gibbs KD Jr. et al. CD47 is an adverse prognostic factor and therapeutic antibody target on human acute myeloid leukemia stem cells. Cell 2009;138(2):286–99. [PubMed: 19632179]
37. Ogilvy S, Metcalf D, Print CG, Bath ML, Harris AW, Adams JM. Constitutive bcl-2 expression throughout the hematopoietic compartment affects multiple lineages and enhances progenitor cell survival. Proc Natl Acad Sci U S A 1999;96(26):14943–14948. [PubMed: 10611317]
38. Todaro GJ, Green H. Quantitative studies of the growth of mouse embryo cells in culture and their development into established lines. J Cell Biol 1963;17:299–313. [PubMed: 13985244]
39. Huang DCS, Cory S, Strasser A. Bcl-2, Bcl-X_L and adenovirus protein E1B19kD are functionally equivalent in their ability to inhibit cell death. Oncogene 1997;14(4):405–414. [PubMed: 9053837]
40. Wu JC, Fritz LC. Irreversible caspase inhibitors: tools for studying apoptosis. Methods in Enzymology 1999;17(4):320–328.
41. Brown MH, Boles K, van der Merwe PA, Kumar V, Mathew PA, Barclay AN. 2B4, the natural killer and T cell immunoglobulin superfamily surface protein, is a ligand for CD48. J Exp Med 1998;188(11):2083–90. [PubMed: 9841922]
42. Waterhouse NJ, Trapani JA. A new quantitative assay for cytochrome c release in apoptotic cells. Cell Death Differ 2003;10(7):853–855. [PubMed: 12815469]
43. O’Reilly LA, Divisekera U, Newton K, Scalzo K, Kataoka T, Puthalakath H, et al. Modifications and intracellular trafficking of FADD/MORT1 and caspase-8 after stimulation of T lymphocytes. Cell Death Differ 2004;11(7):724–736. [PubMed: 15017386]
44. Hibbs ML, Tarlinton DM, Armes J, Grail D, Hodgson G, Maglitto R, et al. Multiple defects in the immune system of *Lyn*-deficient mice, culminating in autoimmune disease. Cell 1995;83(2):301–311. [PubMed: 7585947]

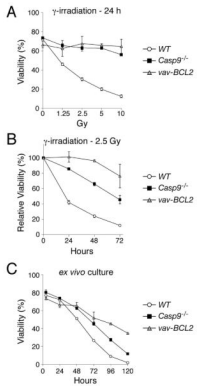

Figure 1. Apoptosis is impaired in *Casp9*$^{-/-}$ thymocytes

Thymocytes of the indicated genotypes were cultured *ex vivo* and, where indicated, exposed to γ-irradiation to provoke apoptosis. Cell viability was determined by staining with PI. The data are presented as means +/− SEM (*WT*, n=8; *Casp9*$^{-/-}$, n=6; *vav-Bcl2*, n=2).

(A), cell viability was measured 24 h after exposure to the indicated doses of γ-irradiation.

(B), cell viability was measured at the indicated times after exposure to 2.5 Gy γ-irradiation, and the data plotted as % viability relative to untreated cells cultured *ex vivo* for the same time.

(C), cell viability was measured after the indicated periods of *ex vivo* culture without cytokine support.

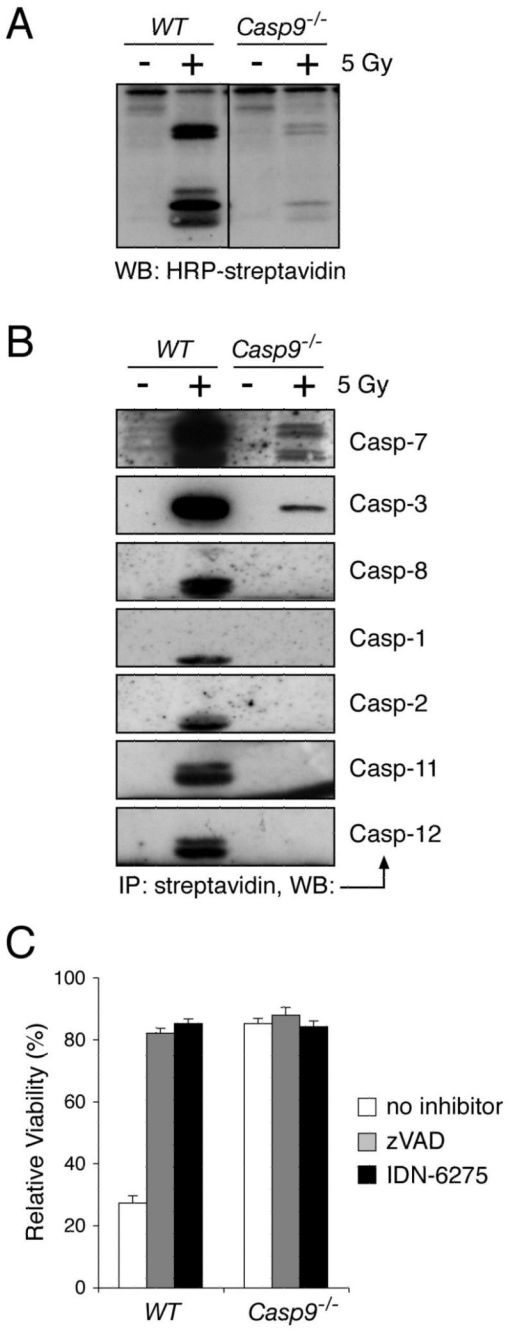

Figure 2. Caspase activation is impaired in *Casp9*$^{-/-}$ thymocytes and contributes little to their ultimate death

(A, B) Lysates were prepared from *WT* and *Casp9*$^{-/-}$ thymocytes that had been either left untreated or exposed to 5 Gy of g-irradiation and then cultured for 8 h. Active caspases were labeled with an irreversible biotinylated caspase inhibitor (biotin-XVAD-fmk, where X is a flexible linker between the biotin and VAD-fmk groups). In (A), the labeled caspases were resolved by SDS-PAGE, and detected by blotting with HRP-streptavidin. In (B), the labeled (active) caspases were purified with streptavidin resin, eluted, resolved by SDS-PAGE and blotted with antibodies recognizing the active subunits of the indicated caspases.

(C) *WT* and *Casp9*$^{-/-}$ thymocytes were either left untreated or exposed to 5 Gy of γ-irradiation and then cultured in the presence of 50 μM zVAD-fmk, 50 μM IDN-6275, or no caspase inhibitor. Cell viability was measured after 24 h by PI staining. The data are shown as % viability of irradiated cells relative to untreated cells cultured for the same time in the presence of the indicated caspase inhibitor to show that the inhibitors do not block the apoptosis induced specifically by the irradiation. The data are presented as means +/− SEM from 3 independent experiments. The absolute cell viabilities measured in these experiments are presented in Fig S3A.

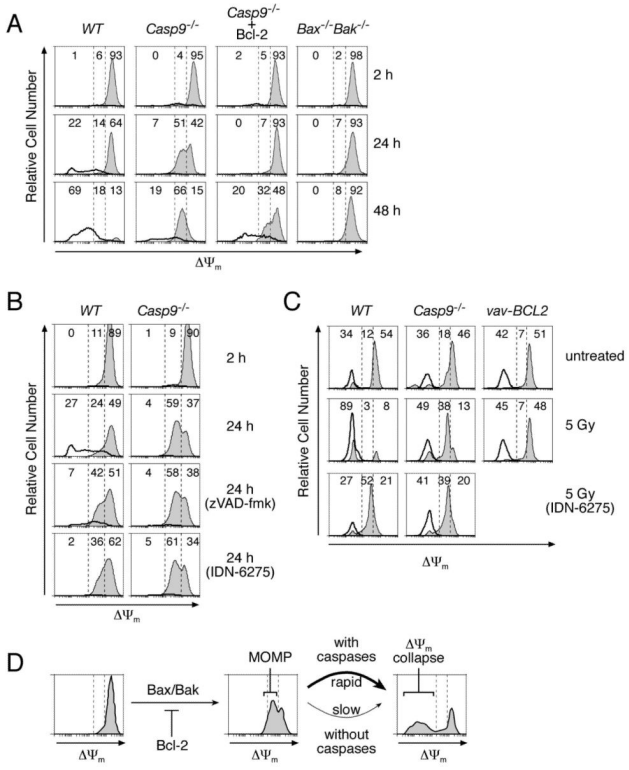

Figure 3. Bcl-2 and caspases control distinct stages of mitochondrial dysfunction

In all panels, the three levels of staining with $DiOC_6(3)$ observed during apoptosis ($\Delta\psi_m^{high}$, $\Delta\psi_m^{intermediate}$ and $\Delta\psi_m^{low}$) are delineated by the dashed vertical lines on the histograms, and the percentages of total cells having each level are indicated. In (A-C), the PI^{-ve} (intact) and PI^{+ve} (dead) cell populations were gated separately; the intact cells were plotted as thin lines with gray fill and the dead cells by a bold line without fill.

(A) *WT*, *Casp9*$^{-/-}$, and *Bax*$^{-/-}$*Bak*$^{-/-}$ MEFs and *Casp9*$^{-/-}$ MEFs stably overexpressing Bcl-2 were exposed to 50 μM etoposide, stained with PI and $DiOC_6(3)$ after the indicated times and analyzed by FACS.

(B) *WT* and *Casp9*$^{-/-}$ MEFs were cultured in the presence of 50 μM etoposide plus 50 μM zVAD-fmk, 50 μM IDN-6275, or no caspase inhibitor. The cells were stained and analyzed as in (A).

(C) *WT*, *Casp9*$^{-/-}$ and *vav-Bcl-2* transgenic thymocytes were either left untreated or exposed to 5 Gy of γ-irradiation and then cultured in the presence of either 50 μM IDN-6275 or no caspase inhibitor for 24 h. The cells were stained and analyzed as in (A).

(D) Model of the observed changes in $\Delta\psi_m$ during apoptosis.

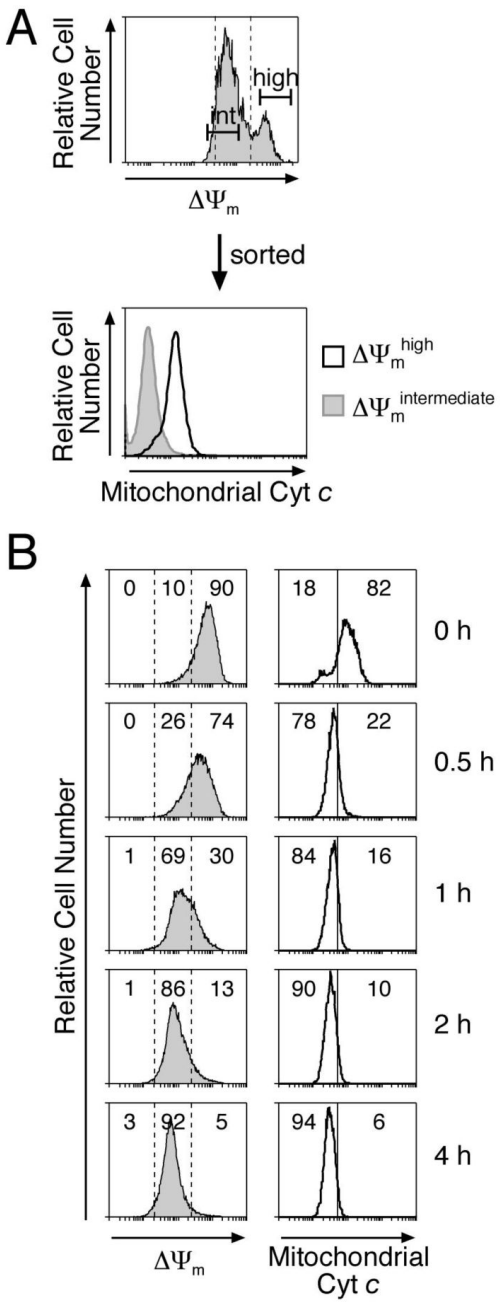

Figure 4. The Bcl-2-regulated drop to intermediate $\Delta\psi_m$ follows MOMP as judged by cytochrome *c* release

(A) *Casp9*$^{-/-}$ MEFs exposed to 50 μM etoposide for 30 h were stained with $DiOC_6(3)$ and sorted into $\Delta\psi_m^{high}$ and $\Delta\psi_m^{intermediate}$ populations, each of which was permeabilized with digitonin to remove cytosolic cytochrome *c*, fixed with formaldehyde and stained with an anti-cytochrome *c* antibody to reveal mitochondrial cytochrome *c* [42].

(B) *Casp9*$^{-/-}$ MEFs stably expressing Noxa were exposed to 2.5 μM ABT-737 and cultured for the indicated times. The cells were either stained with $DiOC_6(3)$ or with an anti-cytochrome *c* antibody as in (A). The percentages of cells in the gated regions of the histograms are indicated. Note that most mitochondrial cytochrome *c* was released by 0.5 h but a comparable drop in DY_m required 1-2 h.

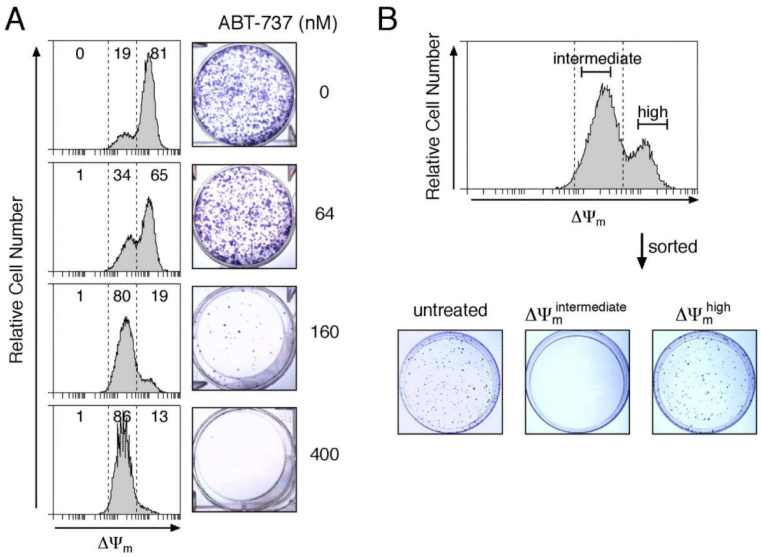

Figure 5. MOMP provokes loss of cell viability in clonogenic assays

(A) *Casp9*$^{-/-}$ MEFs stably expressing Noxa were exposed to the indicated concentrations of ABT-737 for 24 h and then either stained with $DiOC_6(3)$ and analyzed by FACS, or washed, replated and cultured for 7 days to allow colonies to form.

(B) *Casp9*$^{-/-}$ MEFs stably expressing Noxa were exposed to 125 nM ABT-737 for 24 h, stained with $DiOC_6(3)$ and sorted into $\Delta\psi_m^{high}$ and $\Delta\psi_m^{intermediate}$ populations. The sorted cells and untreated control cells were seeded at equal cell densities and cultured for 7 days to allow colonies to form.

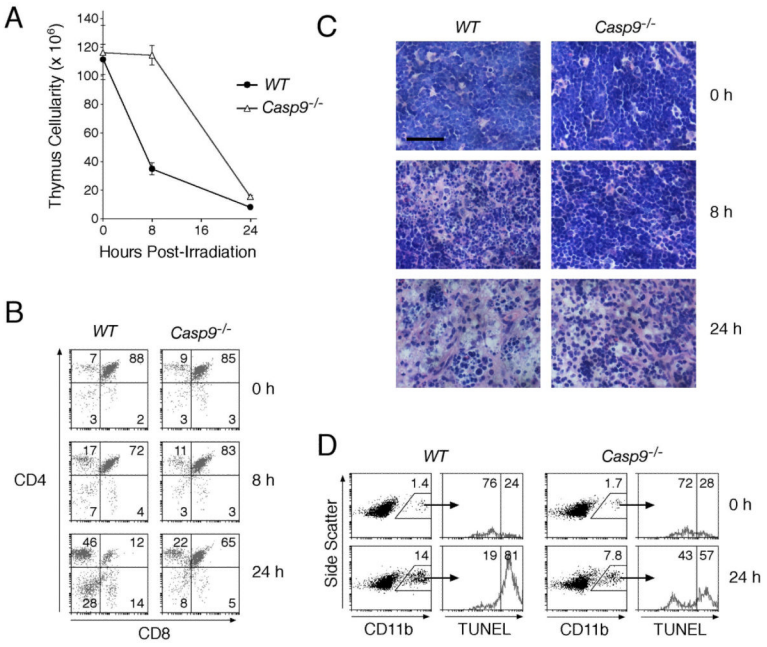

Figure 6. Dying *Casp9*$^{-/-}$ thymocytes are removed by phagocytes *in vivo*, albeit more slowly

Ly5.1 recipient mice whose hemopoietic system had been reconstituted for 11 to 15 wks with fetal liver stem cells from wild-type or *Casp9*$^{-/-}$ Ly5.2 donors were exposed to 5 Gy whole-body γ-irradiation. The mice were sacrificed at 0, 8, and 24 h post-irradiation. n = 3 animals of each genotype at each time point.

(A) Thymic cellularity was determined by enumerating the cells recovered from the harvested thymi. Data are presented as means +/− SEM.

(B) Thymic cell subset composition was determined by staining with anti-CD4 and anti-CD8 antibodies. The percentage of cells in each quadrant is indicated.

(C) Representative hematoxylin and eosin stained sections of thymi at different times post-irradiation. Scale bar = 50 μm.

(D) Cells recovered from the harvested thymi were co-stained with anti-CD11b (Mac1) antibodies and TUNEL. The histograms show TUNEL signal on the gated CD11b^{+ve} cells. The percentages of gated CD11b^{+ve} cells are shown on the dot plots. The histograms indicate the percent of TUNEL^{-ve} and TUNEL^{+ve} cells in the gated CD11b^{+ve} population.

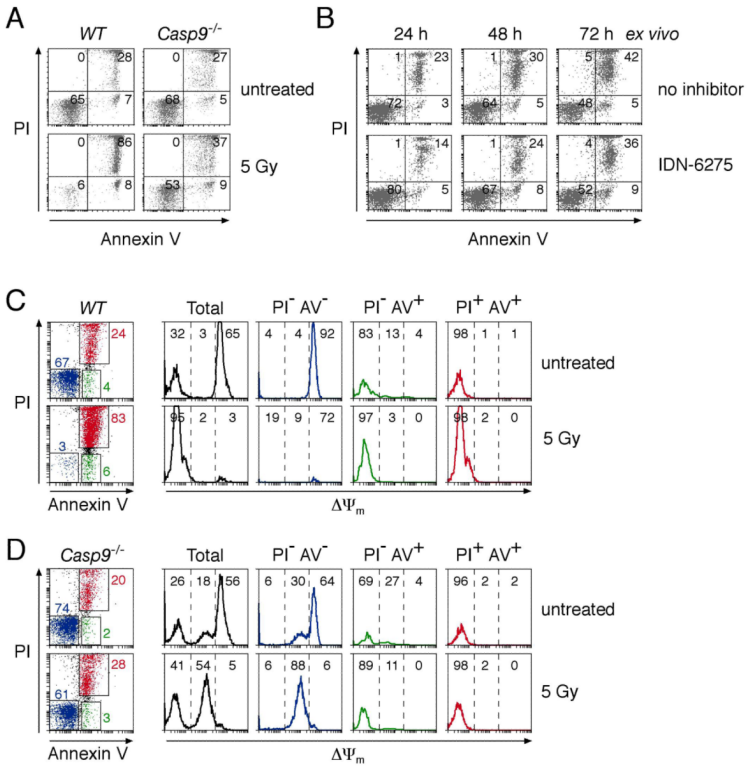

Figure 7. Dying *Casp9*$^{-/-}$ thymocytes expose PS before their plasma membranes become permeable

(A) *WT* and *Casp9*$^{-/-}$ thymocytes were either left untreated or exposed to 5 Gy of γ-irradiation and cultured for 24 h. The cells were then stained with PI and Annexin V and analyzed by FACS. The percentages of cells in each quadrant are indicated.

(B) *Casp9*$^{-/-}$ thymocytes were cultured *ex vivo* in the presence of 50 μM IDN-6275 or no caspase inhibitor. The cells were stained with PI and Annexin V after the indicated periods of culture and analyzed by FACS.

(C, D) *WT* (C) and *Casp9*$^{-/-}$ (D) thymocytes left untreated or exposed to 5 Gy of γ-irradiation were cultured for 24 h and then stained with PI, Annexin V, and $DiOC_6(3)$ and analyzed by FACS. The percentages of cells within each of the gated, color-coded sub-populations are indicated on the dot plots. Histograms representing $\Delta\psi_m$ are plotted for all the cells and each of the gated sub-populations. The histograms are divided into three regions ($\Delta\psi_m^{high}$, $\Delta\psi_m^{intermediate}$, and $\Delta\psi_m^{low}$) defined by the dashed lines and the percentage of the analyzed cells within each region is indicated.

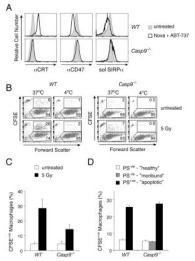

Figure 8. Phagocytes recognize and efficiently engulf dying cells with exposed PS, even *Casp9*$^{-/-}$ ones

(A) *WT* and *Casp9*$^{-/-}$ fibroblasts stably expressing Noxa were either left untreated or exposed for 24 h to 2.5 μM ABT-737, which induces apoptosis in WT fibroblasts and causes *Casp9*$^{-/-}$ fibroblasts to persist in a moribund state with intact plasma membranes and damaged mitochondria (see Figs 4B, S4B). The cells were then stained as indicated with anti-calreticulin antibody, anti-CD47 antibody, or with soluble recombinant SIRPα ectodomain (fused to rat CD4 domains 3 and 4) to demonstrate that the CD47 on the fibroblasts was functional for interaction with its SIRPα receptor.

(B) Untreated and γ-irradiated CFSE-labeled thymocytes were co-cultured with the murine J774 macrophage cell line for 1 h at either 37°C or on ice (4°C). Macrophages (boxed regions) were distinguished from uningested thymocytes (CFSE^{bright} population with low forward scatter) by their large forward scatter (as shown here) or by staining with anti-CD11b antibodies (not shown). The percentages of macrophages that had phagocytosed one or more thymocytes were determined as the % of CFSE^{+ve} macrophages (upper boxed region) relative to the total number of macrophages.

(C) Phagocytosis assays were performed as in (B). The results are presented as means +/− SEM from four independent experiments.

(D) Untreated and γ-irradiated CFSE-labeled thymocytes were sorted into populations enriched with “healthy” (PS^{-ve}, $\Delta\psi_m^{high}$), “moribund” (PS^{-ve}, $\Delta\psi_m^{intermediate}$) or “apoptotic” (PS^{+ve}, $\Delta\psi_m^{low}$) cells. Phagocytosis assays were performed as in (B). The data are presented as means +/− SEM from a representative experiment.

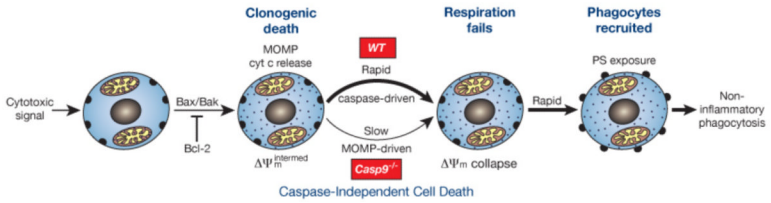

Figure 9. Model for cell death and non-inflammatory corpse removal without caspase activity

Irrespective of caspases, a cytotoxic signal provokes Bax/Bak-driven MOMP and cytochrome *c* release, and the resulting reduction in respiration (reflected in an intermediate $\Delta\psi_m$) imposes clonogenic death. In *WT* cells, the released cytochrome *c* induces rapid caspase-driven $\Delta\psi_m$ collapse, PS exposure and corpse removal by professional phagocytes. In *Casp9*$^{-/-}$ cells, the cells instead linger after MOMP in a moribund state until the impaired respiration leads to $\Delta\psi_m$ collapse, whereupon PS is again rapidly exposed, allowing phagocytes to recognize and engulf the corpse before its plasma membrane becomes permeable. Consequently, even without caspase activity, the cells eventually die and are cleared by non-inflammatory phagocytosis